Passenger kinematics in Lane change and Lane change with Braking Manoeuvres using two belt configurations: standard and reversible

Passenger kinematics in Lane change and Lane change with Braking Manoeuvres using two belt configurations: standard and reversible pre-pretensioner

Ghazaleh Ghaffari, Karin Brolin, Dan Bråse, Bengt Pipkorn,
Bo Svanberg, Lotta Jakobsson and Johan Davidsson

Abstract The development of integrated safety technologies in modern cars demands comprehensive research to predict human occupant response in pre-crash and crash situations. The aim of this study is to investigate occupant kinematics and to provide validation data for Human Body Models (HBMs) in simulations of evasive events potentially occurring prior to a crash. Nine front-seat male passengers, wearing a seat belt in either standard or pre-tensed configuration prior to the event, were exposed to multiple repeatable lane change and lane change with braking manoeuvres while travelling at 73 km/h. The focus of the study was to analyze the occupant kinematics and belt characteristics.

The presented data can be used for validation of HBMs in both sagittal and lateral loading scenarios in simulation of pre-crash events. Corridors comprising mean ± one standard deviation indicated lower sideways and forward displacements for head centre of gravity and T1, with the pre-pretensioner belt versus the standard belt. Upper torso and head lateral excursion were similar for lane change and lane change with braking manoeuvres, while the longitudinal excursions were highly influenced.

Keywords Body kinematics, Human body model, Lane change, Pre-pretensioner belt, Volunteer.

I. INTRODUCTION

Road traffic accidents may have serious health consequences that impose substantial personal and social costs [1]. In order to reduce road traffic injuries, integrated safety technologies that include systems to mitigate accidents and to protect vehicle occupants in a crash have increasingly prevailed in modern cars [2]. For evaluation and further improvement of these safety technologies, it is essential to be able to predict the human occupant response in both pre-crash, e.g. either driver-induced or autonomous braking and steering manoeuvres [3], and crash situations. Human body models (HBMs) are useful mathematical tools to simulate these responses in different loading scenarios [4-7]. In order to understand how representative the models are in evasive manoeuvres and crash events and to develop biofidelic models, they have to be validated with volunteer data in different loading scenarios.

While volunteer data from experiments in sagittal plane loading are available [8-13], fewer studies have investigated volunteer responses in lateral plane loading. Among these studies, Muggenthaler *et al.* [14] established torso kinematics for one helmeted volunteer seated in the passenger seat in a car that drove through a lane change test, and then compared these to the response of Anthropometric Test Devices (ATDs). They found, among other things, that ATDs are not able to predict the human occupants' response in lane change manoeuvres, and therefore that further volunteer studies are necessary. Ejima *et al.* [15] exposed three volunteers, seated in a sled and restrained with a lap belt, to lateral accelerations. Lateral spine flexion was the main motion found in their study. Van Rooij *et al.* [16] studied occupant responses when restrained by a 4-point belt and exposed to simulated lane change manoeuvres in a laboratory test vehicle. They provided

G. Ghaffari (e-mail: ghazaleh.ghaffari@chalmers.se; tel: +46-31-7723652) is a PhD-student, K. Brolin is a Professor and J. Davidsson is an Associate Professor, all at the Department of Mechanics and Maritime Sciences, Chalmers University of Technology, Sweden. D. Bråse and B. Pipkorn are researchers at Autoliv Research, and B. Pipkorn is an Adjunct Professor at Chalmers University of Technology. B. Svanberg is an Attribute Leader and L. Jakobsson is a Senior Technical Leader in Injury Prevention, both at at Volvo Cars, Sweden, and L. Jakobsson is an Adjunct Professor at Chalmers University of Technology.

mainly corridors of head and T1 displacements and reported a significantly greater upper body sideways displacement for relaxed compared to braced subjects. Huber *et al.* [17] performed a series of experiments with volunteers in a modified passenger seat of a car undergoing lane change manoeuvres while measuring head and torso kinematics. In their resultant corridors, an inter-subject variability of above 200% was found for every manoeuvre.

So far, published volunteer studies have provided some understanding of the occupant kinematics and the activity of a limited number of muscles when volunteers were subjected to lateral loading in a laboratory environment. However, none has provided data for volunteers seated in a car travelling in a representative environment. Therefore, experimental data from volunteers travelling in a regular car in a realistic environment, and subjected to repeatable and typical lateral manoeuvres, are needed to validate the HBMs. Further, while new vehicle models are fitted with seat belts that can be pre-tensioned in the pre-crash phase, and these are known to affect the volunteer response in braking events [8-9], no study has investigated these belt configurations in lateral loading scenarios. Hence, the overall objective of the present study is to create a validation dataset for HBMs comprising occupant responses in both sagittal and lateral plane loading through low g interventions using two belt configurations. This paper includes male passenger kinematics in lane change and lane change with braking vehicle manoeuvres using a 3-point seat belt in either activated (henceforth 'pre-pretensioner') or non-activated configuration (henceforth 'standard').

II. METHODS

The use of human volunteers was approved by the Ethical Review Board at the University of Göteborg (application 602-15). The test procedure for each volunteer was that they were: informed about the testing: instrumented as described in the Instrumentation and data acquisition section; and tested in a car on a test track as described in the Test cases section. This paper is part of a larger study on male and female volunteers when exposed to manual and autonomous lane changes, braking, lane changes with braking and U-turn manoeuvres in passenger and driver positions while vehicle dynamics, volunteer-vehicle interaction forces, volunteer's electromyography (EMG) and kinematics are measured.

Volunteers and Inclusion criteria

Volunteers without history of neck pain, poor general health or other medical conditions that could present an increased risk for injury were recruited for this paper (Table A.I, Appendix A). All volunteers gave their informed consent and were compensated with a payment of 800 SEK [76.4 €].

Inclusion criteria were chosen as data with volunteers sitting still and looking forward at the start of each manoeuvre in at least 50% of the manoeuvres, proper functionality of the driving robot mounted in the test vehicle in producing vehicle accelerations within defined limits (i.e. maximum 5.8 m/s^2 lateral acceleration in lane changes and 5 m/s^2 lateral and -5.6 m/s^2 longitudinal acceleration in lane changes with braking), as well as proper functionality of pre-pretensioner belt in producing a predefined level of force (170 N) in time. Three trials were performed per person per type of loading scenario. In total, 92 tests involving nine male volunteers were included in this paper, according to the described criteria.

Test vehicle

The test vehicle was a Volvo V60, model year 2016, with automatic gearbox, summer tyres (Continental SportContact 3 215/50/R17 inflated with 250 kPa) and leather comfort seats. The seat was in its lowest position and seat-back inclination angle was 25°, as measured with Head Restraint Measuring Device. The fore-aft seat position was adjusted to accomplish heel-to-foot plate contact and a knee angle that facilitated comfortable thigh-to-seat cushion contact (Fig. 1). Lumbar support was adjusted to mid position.

Steering and braking interventions were carried out by a driving robot that was developed at Autoliv Research to ensure the repeatability of the passenger manoeuvres. In brief, servomotors,

controlled by a computer placed in the boot of the car, were linked to the steering shaft and the brake pedal to execute the interventions. The test leader, positioned in the rear seat, uploaded executable files to the robot computer via a personal computer. The interventions were initiated by the test leader via a data acquisition and control computer (SIRIUS SBOX computer) that sent a trigger signal to the robot computer.

Reversible pre-pretensioner seatbelt (Autoliv, Stockholm, Sweden), controlled by the SIRIUS SBOX computer via an interface (VN1640, Vector GmBH, Stuttgart, Germany) was installed in the vehicle. When activated, the belt pull-in was initiated at around 200 m/s prior to the onset of lateral loading (time zero) in an autonomous intervention and applied a target force of 170 N. The target force was reached at approximately 400 m/s after the defined time zero (Fig. C.1. in Appendix). Before each new test, the full length of the belt was manually pulled out and in to ensure representative seat-belt characteristics and initial belt position on the volunteer. When inactivated, i.e. 'standard', no pre-tension was applied.

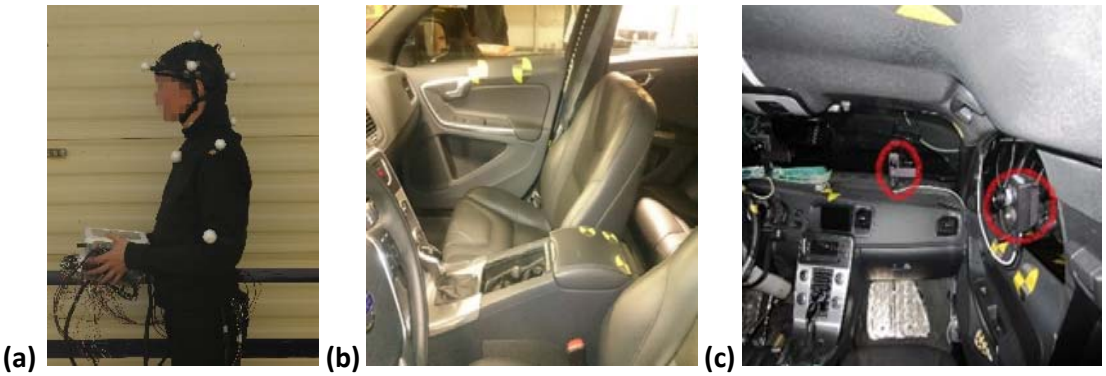

Fig. 1. (a) Volunteer prepared for test, (b) passenger seat position, (c) interior of test vehicle presenting side and front cameras, foot plates for the passengers and photo targets.

Test cases

Four types of loading scenarios were to some extent randomly repeated three times for each volunteer within a larger test series comprising a total of 18 scenarios in both passenger and driver positions. This paper presents passenger data from autonomous lane change and autonomous lane change with braking manoeuvres with the standard and the pre-pretensioner seat belt. The lane change with standard belt is denoted LSB, the lane change with braking and with standard belt is denoted LBSB, the lane change with pre-tensioner belt is denoted LPT, and the lane change with braking and with pre-tensioner belt is denoted LBPT.

At the initial vehicle velocity used in this study, 73 km/h, a lane change manoeuvre produced a maximum lateral acceleration of 5.8 m/s^2, while a lane change with braking manoeuvre produced a maximum lateral acceleration of 5 m/s^2 and a longitudinal acceleration of -5.6 m/s^2 (Fig. 2). The subject was unaware of the type and, to some extent, the onset time of the scenario. Vehicle roll, pitch and yaw angles are shown in Fig. B.1 (Appendix). Maximum change in vehicle yaw angle was on average 12.4° for the LSB/LPT and 12° for the LBSB/LBPT.

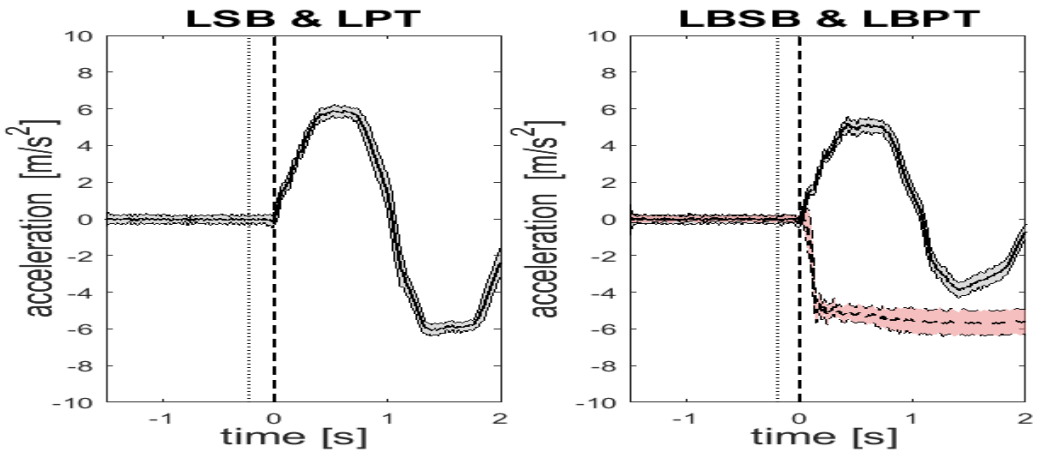

Fig. 2. Lateral vehicle acceleration (solid grey) in LSB & LPT and lateral and longitudinal vehicle acceleration (solid grey and dashed pink, respectively) in LBSB & LBPT. Vertical dashed lines present time zero and vertical dotted lines present the onset time of the pre-tensioned belt, n = 25, 23, 24 and 20 for LSB, LPT, LBSB and LBPT, respectively.

Instrumentation and data acquisition

The volunteer's motion was captured with three DS-CAM 600 cameras (DEWESoft d.o.o., Slovenia) connected to a SIRIUS SBOX computer via a CAM-BOX3 (DEWESoft d.o.o., Slovenia) using wide-angle lenses at 50 f/s and with a resolution of 1280×1080. Cameras were positioned to capture occupant motion from forward (focal length 6 mm), rearward (focal length 4.5 mm) and side (focal length 6 mm) (Fig. 1). White and lightweight spheres, 25 mm in diameter, were attached to the volunteer to provide 3-D information for kinematics post-processing. Five spheres were attached to the volunteer's head using a system of straps (Fig. 1); total weight of straps and spheres was 52 g. Single spheres were attached to the skin covering the T1 process, the sternum and left and right acromion, respectively, all located by palpation. Spheres were also strapped to the distal part of the upper arm. Several flat photo targets were attached to the interior of the vehicle for referencing. In addition and prior to each series of tests, an array of spheres, referred to as calibration plate, with known positions in the vehicle space, were positioned in the seat and videos were collected to enable the establishment of a common reference system.

Shoulder- and lap-belt forces were recorded using two low load belt force sensors (Entran EL20-5kN) mounted to belt segments to the right of the volunteer. Belt pay-out was measured using an optical belt movement sensor. Feet-to-vehicle interaction forces in the car were measured using three axis load cells (Denton 2358FL) mounted between foot plates (Fig. 1) and the car chassis. The passenger right and left foot plates were angled 47° relative to horizon. All aforementioned signals were sampled at 20 kHz by the data acquisition system included in the SIRIUS SBOX computer and a SIRIUS ACC unit connected to the SIRIUS SBOX computer. Pressure distribution between the volunteer and the seat cushion was measured using a pressure-sensitive mattress, 471.4 mm x 471.4 mm, that included 1,024 evenly distributed pressure sensors (CONFORMat Sensor 5330, version 7.60-30I, Tekscan, Inc., Boston, USA). The sensors were connected via a VersaTek 8-port Hub to a personal computer. Trigger signals sent from the SIRIUS SBOX computer facilitated timely pressure recordings. Vehicle GPS position and kinematics were recorded at 100 Hz using a roof-mounted inertial measurement unit (DS-IMU2, DEWESoft d.o.o., Slovenia) that was connected to the SIRIUS SBOX computer. Steering-wheel angle was collected from the CAN-bus at 100 Hz.

Data analysis

Data was analysed by MATLAB v.2015a provided by Mathworks Inc.

The vehicle acceleration data were smoothed using a 3rd-order Butterworth low-pass filter with 20 Hz cut-off frequency, and then compensated for vehicle angular accelerations to estimate mid-vehicle acceleration at approximately the occupant H-point height and fore-aft location. For each manoeuvre, the onset of the test, also referred to as time zero, was defined as 200 m/s before the lateral vehicle acceleration reached 55% of its maximum. This time scaling results in synchronised acceleration data collected in all included tests and a common definition of time zero where the lateral acceleration is approximately zero (Fig. 2).

Film analysis and kinematics post-processing

A 3D film analysis of the data from the front, side and rear cameras was performed using TEMA Automotive (Image Systems, Linköping, Sweden). Image distortion due to the wide-angle lenses was compensated by lens calibration according to the protocol provided in TEMA Automotive. In order to calculate the orientation of the cameras, and thus a single coordinate system for the three camera views, the videos collected from the calibration plate positioned in the seat prior to each volunteer's series of tests were used according to a TEMA protocol. The established coordinate systems were according to Fig. 3a, but with the origin in the centre of the calibration plate. After film analysis, the provided coordinates of the markers attached to the volunteer's head and torso were used to calculate the head rotation angles, the excursion of a point approximately at the head centre of gravity (CoG) and a point close to the T1 vertebra body with respect to the vehicle coordinate system in 3D. The accuracy of the video-tracking was found to be within 10 mm deviation from the average distance between each of the two markers attached to the head.

Euler angles

The extrinsic Euler angles, via Tait-Bryan convention $Z_1Y_2X_3$, were calculated for the head and the upper torso, using coordinates of the three best trackable markers attached to the corresponding presumably rigid body (typically, one marker on forehead and two markers on right and left sides of head, and single markers on left acromion, T1 process and sternum), with respect to the fixed coordinate system. The rotations around Z-, and the updated Y- and X-axis, are referred to as yaw, pitch and roll, respectively (Fig. 3(a)). Both head and upper torso rotation matrices were constructed in a similar fashion using Equation 1, where ***A*** and ***B*** matrices (*P* stands for point) were composed given the coordinates of the three markers, while ***A*** was ***B*** at the defined time zero.

$$\boldsymbol{B} = \boldsymbol{R}\,\boldsymbol{A} \Rightarrow \boldsymbol{R} = \boldsymbol{B}\,\boldsymbol{A}^{-1},\ \boldsymbol{A} = \begin{bmatrix} P_{1x,t0} & P_{2x,t0} & P_{3x,t0} \\ P_{1y,t0} & P_{2y,t0} & P_{3y,t0} \\ P_{1z,t0} & P_{2z,t0} & P_{3z,t0} \end{bmatrix}, \boldsymbol{B} = \begin{bmatrix} P_{1x,ti} & P_{2x,ti} & P_{3x,ti} \\ P_{1y,ti} & P_{2y,ti} & P_{3y,ti} \\ P_{1z,ti} & P_{2z,ti} & P_{3z,ti} \end{bmatrix} \quad \text{(Eq. 1)}$$

Implementing the extrinsic rotation sequence using three elemental rotations led to the achievement of an analytical rotation matrix (Eq. 2), and then equating the analytical with measured rotation matrix yielded the rotation angles around Z-, Y- and X-axis, denoted by φ, θ and ψ, respectively.

$$\boldsymbol{R}_{analytical} = \boldsymbol{R}_z(\phi)\,\boldsymbol{R}_y(\theta)\boldsymbol{R}_x(\psi) = \begin{bmatrix} \cos\phi\cos\theta & \cos\phi\sin\theta\sin\psi - \cos\psi\sin\phi & \sin\phi\sin\psi + \cos\phi\cos\psi\sin\theta \\ \cos\theta\sin\phi & \cos\phi\cos\psi + \sin\phi\sin\theta\sin\psi & \cos\psi\sin\phi\sin\theta - \cos\phi\sin\psi \\ -\sin\theta & \cos\theta\sin\psi & \cos\theta\cos\psi \end{bmatrix} \quad \text{(Eq. 2)}$$

Head centre of gravity (CoG)

Head CoG coordinates were calculated in 3D using Equation 3:

$$\boldsymbol{Head}_{CoG} = \boldsymbol{P}_{side} + \boldsymbol{R}(\psi, \theta, \phi)(\boldsymbol{M} + \boldsymbol{r}) \quad \text{(Eq. 3)}$$

where $\boldsymbol{P}_{side}$ was coordinates of the marker on the left side of passenger's head, ***R*** was the 3D rotation matrix, ***M*** was a position vector measured for each volunteer while Frankfort (FF) plane was aligned with the horizontal plane (θ_{FF}= 0, M_x and M_z were horizontal and vertical distances from $\boldsymbol{P}_{side}$ to the auditory canal (rear FF-plane) and M_y was equal to half of the head width plus the radius of the sphere marker and the length of its holder), and ***r*** was the position vector of the CoG in the head anatomical coordinate system. The components of ***r*** for a male were chosen as r_x = 8.7 mm, r_y = 0 and r_z = -26.8 [18-20], assuming the head CoG is located at no offset in head anatomical y-axis (Fig. 3(b)).

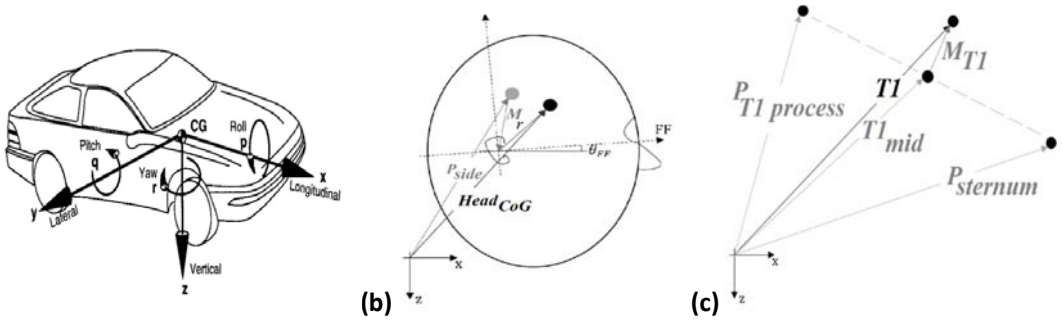

(a) **(b)** **(c)**

Fig. 3. (a) The coordinate system in the test vehicle [21], while a slightly different origin was used for each volunteer, (b) schematic view of the vectors required to calculate the head CoG coordinates with respect to the vehicle coordinate system, (c) schematic view of the vectors required to calculate the T1 coordinates with respect to the vehicle coordinate system.

T1 vertebra level

T1 coordinates were calculated in 3D using Equation 4:

$$\boldsymbol{T1} = \boldsymbol{T1}_{mid} + \boldsymbol{R}(\psi, \theta, \phi) \cdot \boldsymbol{M}_{T1} \quad \text{(Eq. 4)}$$

where $\boldsymbol{T1}_{mid}$ was the average coordinates of the markers on the skin of T1 process ($\boldsymbol{P}_{T1\ process}$) and the sternum ($\boldsymbol{P}_{sternum}$) in the vehicle coordinate system, ***R*** was the 3D rotation matrix and $\boldsymbol{M}_{T1}$ was the measured position vector from $\boldsymbol{T1}_{mid}$ to T1 vertebra level by aligning a schematic of a generic skeleton with the volunteer's image ($M_{T1\,x}$ and $M_{T1\,z}$ were horizontal and vertical distances and $M_{T1\,y}$ =0), see Fig. 3(c).

III. RESULTS

For each loading scenario vehicle dynamics, including lateral and longitudinal accelerations (Fig. 2), and roll, pitch and yaw angles (Fig. B.1, Appendix), shoulder- and lap-belt interaction forces (Fig. C.1, Appendix) and volunteer kinematics corridors (Fig. 5, Fig. 6, and also Fig. D.1 to Fig. D.6 in Appendix), were established using mean and mean ± one standard deviation (S.D.) with n = 25, 23, 24 and 20 for LSB, LPT, LBSB and LBPT, respectively. Front- and side-view snapshots (Fig. 4) and the pressure distributions on the passenger seat (Fig. E.1, Appendix) for a representative male passenger in a LSB manoeuvre are presented for clarification of the results.

Kinematics

As the car steers to the right in a LSB manoeuvre, the head and upper torso translate towards the centre of the car (Fig. 4, t=0.5 s) and the pressure on the passenger seat is more left side distributed (Fig. E.1, t=0.5 s). Thereafter, torso and head move slowly towards the initial positions (Fig. 4, t=1 s) and pressure on the seat is more evenly distributed (Fig. E.1, t=1 s), although the lateral acceleration is still applied. In the 1–1.5 s interval, as the car steers to the left, the head and torso translate to the right (Fig. 4, t=1.5 s) and pressure on the seat is more right side distributed (Fig. E.1, t=1.5 s). The

volunteer returns to almost initial position in the 1.5–2 s interval, although some lateral acceleration is still applied to the body. According to pressure distribution on the passenger seat (Fig. E.1, Appendix), pelvis forward displacement was found to be negligible.

t = 0 s t = 0.5 s t = 1 s t = 1.5 s t = 2 s

Fig. 4. Video data in one LSB manoeuvre (male 3); front view (top row) and lateral view (bottom row) for five points in time.

For LSB scenario, corridors of head CoG displacement in x-, y- and z-axis are illustrated in Fig. 5 (left panel). Corridors of head rotation angles, i.e. roll, pitch and yaw, are illustrated in Fig. 5 (right panel). As shown in Fig. 5, head CoG appears to have major displacement in y-axis compared to x- and z-axis. Corridors of T1 displacement in x-, y- and z-axis are illustrated in Fig. 6. Again, the major T1 displacement is found in y-axis and its direction is consistent with head sideway displacement. Note that when the volunteer moves to the left as the vehicle steers to the right, the upper torso turns counter-clockwise, i.e. towards left, while the head turns slightly clockwise towards right, and vice versa when the vehicle steers to left.

Comparing corridors of head and torso kinematics in LSB (Fig. 5 and Fig. 6, respectively) with same corridors in LPT (Fig. D.1 and Fig. D.2, Appendix) indicates that in the first second of the manoeuvres, volunteers have less head and T1 sideway displacement in LPT (max. 96 mm for head and 66 mm for T1) than in LSB (max. 152 mm for head and 130 mm for T1). Same comparison between corridors in LBSB (Fig. D.3 and Fig. D.4, Appendix) and corridors in LBPT (Fig. D.5 and Fig. D.6, Appendix) results in less head and T1 sideway displacement found in LBPT (max. 87 mm for head and 67 mm for T1) than in LBSB (max. 155 mm for head and 135 mm for T1).

Head and T1 forward displacement was found less in LBPT (max. 91 mm for head and 41 mm for T1) than in LBSB (max. 114 mm for head and 65 mm for T1) compared to corresponding corridors. In all loading conditions, T1 had less sideway and forward displacement than head CoG. Head and torso displacement in z-axis shows no noticeable difference between LSB and LPT nor between LBSB and LBPT. Head rotation angles did not reveal noticeable differences between those loading conditions.

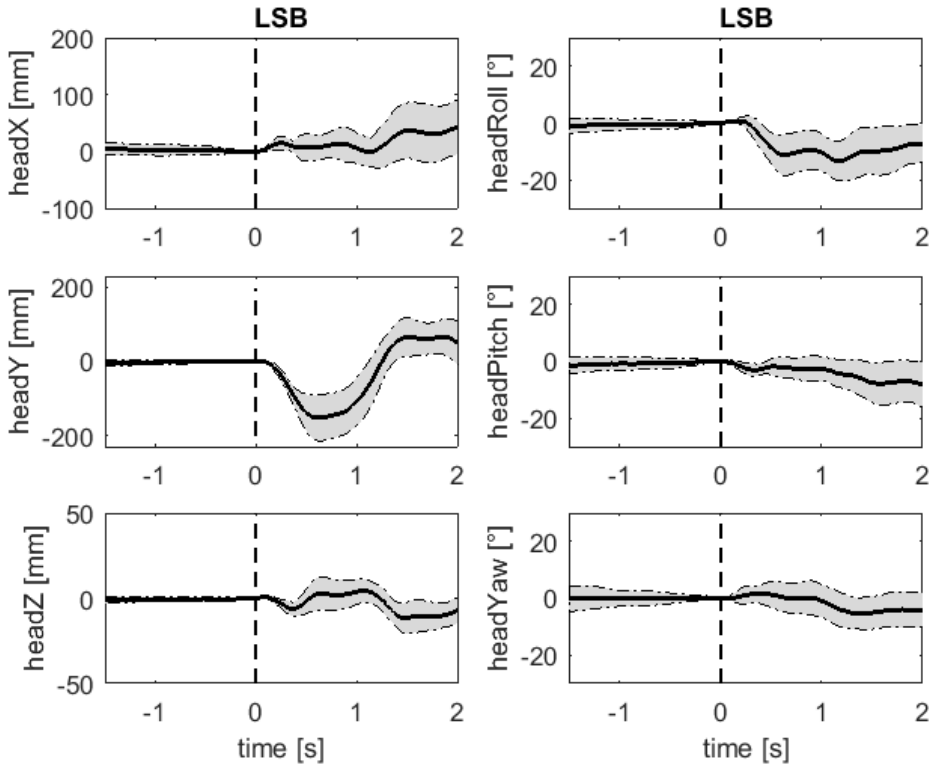

Fig. 5. Head kinematics in LSB, vertical dashed lines present time zero, n=25.

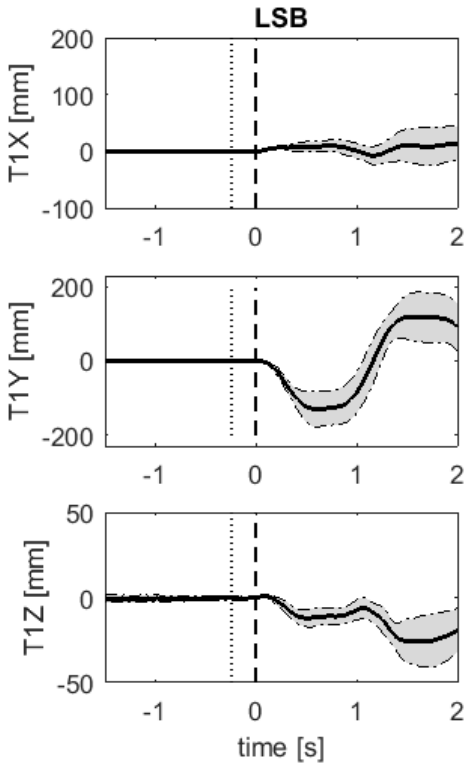

Fig. 6. Upper torso kinematics in LSB, vertical dashed lines present time zero, n=25.

IV. DISCUSSION

In this paper, a series of manoeuvres, such as lane change and lane change with braking, was conducted. The aim was to assess the vehicle occupants' responses to potential pre-crash situations and to create validation data for HBMs capable of controlling muscle activation. All manoeuvres were conducted with two belt configurations separately, standard belt and pre-pretensioner belt, to allow for comparison and investigation of the pre-tensioning effects on occupants' responses. Passengers' kinematics were quantified and presented in corridors of mean ± S.D. for head CoG and T1 displacements in 3D and head rotations around three axes. Corridors of vehicle acceleration, roll, pitch and yaw, as well as shoulder- and lap-belt interaction forces and belt pay-out data were presented as the boundary conditions required for the HBMs' validation.

Advantages and limitations

The use of a test vehicle outdoors, instead of a sled setup indoors, had advantages and disadvantages. Although the type of vehicle used in this study was not representative of all vehicle types and the tests were not done in regular traffic situations, the vehicle-based experiment certainly provided more realistic data than sled tests performed in a laboratory. On the other hand, one disadvantage of using a test vehicle was the limited space in combination with structures that obstructed the view of the pelvis and the lower extremities. Hence, obtaining detailed kinematic data for these body regions was challenging and therefore they were not included in this paper. In addition, strong sun-light, as well as low light on cloudy days, posed other challenges during video recording and occasionally resulted in poor video quality. Additionally, rain could affect the functionality of the autonomous braking and lane change manoeuvres in producing accurate and repeatable accelerations; this kind of error was accounted for by detailed analysis of the vehicle acceleration. Individual acceleration data were assessed and no noticeable difference was found in lateral acceleration of the included test data when the tests were performed in dry conditions as opposed to on wet pavements.

In this study, all manoeuvres with initial vehicle speed of 73 km/h were performed randomly and repeated three times for each volunteer. The aim of this random testing was to reduce the risk of systematic errors caused by, for instance, habituation in one specific manoeuvre. According to Bluoin *et al.* [22], volunteers can modify their muscle responses when they are exposed to repeated analogous acceleration impulses. This habituation behaviour might also exist in volunteers' kinematics, but it was not investigated among the three repetitions of each loading scenario in this study; it could be subject to further statistical analyses. Furthermore, although the tests were arranged so that all volunteers were unaware of upcoming manoeuvres, the possibility of volunteers being aware of it cannot be ruled out in some data. For instance, it is possible that the sound produced by the clutch, which was engaged by the robot prior to the execution of the manoeuvre and which was located underneath/forward of the driver seat, acted as a forewarning. If a volunteer is aware of the coming manoeuvre, this can affect the muscle responses as well as kinematics; in this study we did not compensate our results for this potential error. To provide more accurate and representative kinematics responses, all individual data were assessed with respect to the initial head and torso postures and those that were not at neutral postures, i.e. sitting still and looking forward, within 0.5 s prior to the start of the manoeuvres were excluded. This allowed us to investigate the effect of the pre-tensioner belt on volunteers' responses when there was no major voluntary motion just prior to the start of the manoeuvres.

In the data analysis, time scaling was based on the onset of lateral acceleration as it is likely the most accurate indication of the beginning of the event, that is, it is likely the first indicator of a manoeuvre detectable by the volunteer, with the exception of belt motion in LPT and LBPT tests, rather than using the steering-wheel angle as in other, similar studies [17]. In a study conducted by Huber *et al.* [17], the steering wheel seemed to begin turning at around 130 m/s prior to the generated lateral acceleration, which could be due to limited steering angle change rate, deck slip, and activation of the suspension system due to vehicle inertia. Accordingly, it can be different for

different vehicle models. One disadvantage of using acceleration instead of steering-wheel angle could be that the steering-wheel rotation might affect the awareness of the volunteer; although this time delay was found to be less than 50 ms max. in the performed manoeuvres – except for LPT, in which the maximum time delay was less than 100 ms. The effect of this delay on our study is unknown.

Volunteers were exposed to lane change and lane change with braking manoeuvres while travelling at 73 km/h. This velocity was chosen to facilitate significant lateral vehicle accelerations in lane changes and at the same time deemed safe.

Kinematic responses

Results showed that there were some variabilities in volunteers' responses, especially for head kinematics, that led to broader corridors than for T1 kinematics. This suggests that the inter-individual differences are deemed to be important. In lane change manoeuvres, the main displacement seen for head and T1 was the same sideway motion. Similarly, in the lane changes with braking, the main displacement seen for head and T1 were sideway and forward motions. Head showed slightly larger displacements than T1 in all types of loading scenarios comparing the mean corridors. In general, corridor shapes were similar in lane changes with two belt configurations, but with quantifiable differences in amplitude. Lane changes with pre-pretensioner belt were characterised with lower head and T1 sideway and forward mean displacement compared to lane changes with standard belt. These findings suggest that the pre-pretensioner belt plays an important role in reducing the volunteer's motion during the pre-crash situations.

The statistical significance of the presented comparison between manoeuvres with standard and pre-pretensioner belt (i.e. volunteer's kinematics in LSB vs LPT/LBSB vs LBPT) has not been investigated in this paper. Hence, in order to determine the effects of pre-pretensioner belt on body motions, further studies will be required to assess the significance of the observed differences.

Studies on female volunteer data and the gender differences in volunteer responses are also essential and necessary for the development of female models. Particularly, due to physiological differences, gender might be a factor that affects the muscle responses, body kinematics and volunteers' behavior in response to various loading scenarios. The current work focuses only on the data from the male participants and the collected female data are planned to be analyzed and presented in a future paper.

In calculation of Tait-Bryan rotation angles, an underlying assumption was that this method is applied to a rigid body. Although the head is a rigid body in essence, the upper torso is not. Hence, an error is introduced when the upper torso rotation matrix is used in the calculation of the upper torso linear displacements (Equation 4). However, the vector (M_{T1}) is small and the resulting contribution of linear displacement from the rotation of the upper torso is small compared to the motion of the photo targets attached to the skin covering the T1 process and Sternum. Therefore the upper torso linear displacements are presented while upper torso rotational displacements are not.

The kinematics results presented here cannot be compared with previous studies because none of them had the same boundary conditions as this study. However, upper torso sideway motion was commonly found as one of the main body motions both in this paper and in previous studies in lateral loading [15-17]. Furthermore, it has been confirmed that muscle activation can affect body posture and kinematics in a crash event, to some degree [23-24], and in a pre-crash situation, to an even greater extent, due to a longer duration and lower loads than in crash events [8]. In order to relate body postures and kinematics with muscle activities, analysis of electromyography data is needed. This was not included in the present paper, although it was collected and is available for inclusion in future studies. Studying volunteers' muscle activation in addition to their kinematics will increase the capacity of HBMs to mimic muscle responses in conjunction with body postures.

V. CONCLUSION

This study focused on body kinematics data recorded from nine male passengers during autonomous lane change and lane change with braking, using two belt configurations, i.e. standard and pre-pretensioner. A detailed set of validation data for the HBMs was provided, comprising corridors of head CoG and upper torso displacement and head rotations around three axes, as well as boundary conditions, such as interaction forces and vehicle dynamics. Comparisons of the two belt configurations suggested lower sideway and forward displacements for head and T1, with the pre-pretensioner belt versus the standard belt, based on mean corridors. By the means of HBMs validated by human responses, the possibility of predicting human kinematics in pre-crash scenarios will increase and will enhance the models' ability to help improve the design of integrated safety systems in modern cars.

VI. ACKNOWLEDGEMENTS

The authors would like to specially thank all participants in the tests, and our colleagues Rustem Elezovic at Autoliv Research AB, Jonathan Fahlbeck, Sofia Johansson, Oscar Cyrén and Sumit Sharma at Chalmers and Per Lindén and Johan Svensson at Volvo Cars. The work was carried out at SAFER-Vehicle and Traffic Safety Centre at Chalmers, Gothenburg, Sweden, and funded by FFI-Strategic Vehicle Research and Innovation, by Vinnova, the Swedish Energy Agency, the Swedish Transport Administration and the Swedish vehicle industry.

VII. REFERENCES

[1] http://www.who.int/violence_injury_prevention/road_safety_status/2015/en/ Accessed 29 March 2018.

[2] EC FP7 ASSESS – Assessment of Integrated Vehicle Safety Systems for Improved Vehicle Safety. SST 2nd Call, Grant Agreement No. 233942. Available from: http://www.assess-project.eu. Accessed 29 March 2018.

[3] Unselt, T., *et al*. (2011) Assessment of behavioural aspects in integrated safety systems (EU FP7 project ASSESS). *Enhanced Safety of Vehicles (ESV) Conference Proceedings*, 2011, Washington D.C., paper no. 11-0284.

[4] Iwamoto, M., Nakahira, Y., Kimpara, H., Sugiyama, T., Min, K. (2012) Development of a human body finite element model with multiple muscles and their controller for estimating occupant motions and impact responses in frontal crash situations. *Stapp Car Crash Journal*, **56**: pp. 231–68.

[5] Östh, J., Brolin, K., Bråse, D. (2015) A Human Body Model With Active Muscles for Simulation of Pretensioned Restraints in Autonomous Braking Interventions. *Traffic Injury Prevention*, **16**(3): pp. 304–13.

[6] Subit, D., Möhler, F., Wass, J., Pipkorn, B. (2016) Robustness of Principal and Longitudinal Strains as Fracture Predictors in Side Impact. *Proceedings of the IRCOBI Conference*, 2016, Malaga, Spain.

[7] Östh, J., Brolin, K., Carlsson, S., Wismans, J., Davidsson, J. (2012) The occupant response to autonomous braking: A modeling approach that accounts for active musculature. *Traffic Injury Prevention*, **13**(3): pp. 265–77.

[8] Östh, J., Olafsdóttir, J. M., Davidsson, J., Brolin, K. (2013) Driver kinematic and muscle responses in braking events with standard and reversible pre-tensioned restraints: validation data for human models. *Stapp Car Crash J.*, **57**: pp. 1–41.

[9] Ólafsdóttir, J. M., Östh, J., Davidsson, J., Brolin, K. (2013) Passenger kinematics and muscle responses in autonomous braking events with standard and reversible pre-tensioned restraints. *Proceedings of the IRCOBI Conference*, 2013, Gothenburg, Sweden, pp. 602–17.

[10] Ejima, S., Ono, K., Holcombe, S., Kaneoka, K., Fukushima, M. (2007) A study on occupant kinematics behaviour and muscle activities during pre-impact braking based on volunteer tests. *Proceedings of IRCOBI Conference*, 2007, Maastricht, the Netherlands, pp. 31–45.

[11] Behr, M., *et al*. (2010) Posture and muscular behaviour in emergency braking: An experimental approach. *Accident Analysis and Prevention*, **42**(3): pp. 797–801.

[12] Ejima, S., Zama, Y., Satou, F., Holcombe, S. (2008) Prediction of the physical motion of the human body based on muscle activity during pre-impact braking. *Proceedings of IRCOBI Conference*, 2008, Bern, Switzerland, pp. 163–75.

[13] Choi, H. Y., *et al*. (2005) Experimental and numerical studies of muscular activations of bracing occupant. *Proceedings of 19th ESV Conference*, 2005, Washington, D.C., paper no. 05-0139.

[14] Muggenthaler, H., Adamec, J., Praxl, N., Schönpflug, M. (2005) The influence of muscle activity on occupant kinematics. *Proceedings of the IRCOBI Conference on the Biomechanics of Impact*, 2005, Prague, Czech Republic.

[15] Ejima, S., *et al*. (2012) Effects of pre-impact swerving / steering on physical motion of the volunteer in the low-speed side-impact sled test. *Proceedings of the IRCOBI Conference on the Biomechanics of Impact*, 2012, Dublin, Ireland.

[16] van Rooij, L., Elrofai, H., Philippens, MMGM., Daanen, HAM. (2013) Volunteer Kinematics and Reaction in Lateral Emergency Maneuver Tests. *Stapp Car Crash Journal*, **11**(57): pp. 313–42.

[17] Huber, P., Kirschbichler, S., Pruggler, A., Steidl, T. (2015) Passenger kinematics in braking, lane change and oblique driving maneuvers. *Proceedings of the IRCOBI Conference*, 2015, Lyon, France.

[18] Beier, G., *et al.* (1980) Center of gravity and moments of inertia of human heads. *Proceedings of the IRCOBI Conference*, 1980, Birmingham, England, pp. 218–28.

[19] Walker, L. B., Harris, E. H., Pontius, U. R. (1973) Mass, volume, center of mass, and mass moment of inertia of head and head and neck of human body. *Proceedings of the Stapp Car Crash Conference*, 1973, Society of Automotive Engineers, Warrendale, PA, pp. 525–37.

[20] Yoganandan, N., Pintar, F., Zhang, J., Baisden, J. L. (2009) Physical properties of the human head: mass, center of gravity, and moment of inertia. *Journal of Biomechanics,* **42**(9): pp.1177–92.

[21] Evangelos, Ch. Tsirogiannis. (2015) Design of an efficient and lightweight chassis, suitable for an electric car. Thesis for: M.Eng, National Technical University of Athen, 2015, DOI10.13140/RG.2.2.30711.21920.

[22] Blouin, J. S., Descarreaux, M., Bélanger-Gravel, A., Simoneau, M., Teasdale, N. (2003) Attenuation of human neck muscle activity following repeated imposed trunk-forward linear acceleration. *Experimental Brain Research*, **150**(4), pp. 458–64.

[23] Hendler, E., *et al*. (1974) Effect of head and body position and muscular tensing on response to impact. *Proceedings of the Stapp Car Crash Conference*, Society of Automotive Engineers, Warrendale, PA, pp. 303–37.

[24] Begeman, P. C., King, A. I., Levine, R. S., Viano, D. C. (1980) Biodynamic response of the musculoskeletal system to impact acceleration. *Proceedings of the Stapp Car Crash Conference*, 1980, Society of Automotive Engineers, Warrendale, PA, pp. 479–509.

VIII. APPENDIX

Appendix A

Age and anthropometric data of the volunteers included in this study are presented in Table A.I.

TABLE A.I

VOLUNTEER AGE AND ANTHROPOMETRICS

Volunteer	Age (Years)	Stature (cm)	Weight (kg)	Sitting height (mm)
Male 1	35	174	63	940
Male 2	23	184	78	960
Male 3	42	179	68	930
Male 4	25	192	65	960
Male 5	23	183	77	948
Male 6	71	178	71	894
Male 7	40	180	65	990
Male 8	26	185	79	973
Male 9	26	192	85	964
Mean	34.6	183	72.3	951
Std.	15.5	6.1	7.7	27.7

Appendix B

Vehicle's roll, pitch and yaw angles are shown for LSB/LPT and LBSB/LBPT manoeuvres in Fig. B.1.

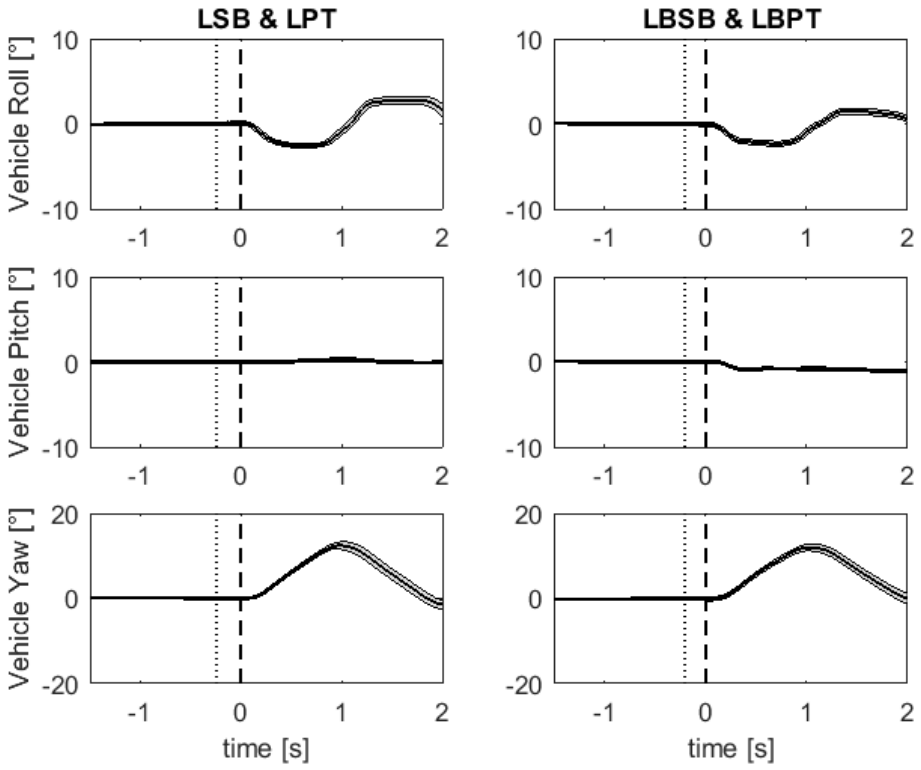

Fig. B.1. Vehicle angular displacement in LSB & LPT (left panel) and in LBSB & LPBT (right panel). Vertical dashed lines present time zero and vertical dotted lines present the onset time of the pre-tensioned belt, n = 25, 23, 24 and 20 for LSB, LPT, LBSB and LBPT, respectively.

Appendix C

Shoulder-belt and lap-belt interaction forces, as well as belt pay-out, are illustrated for LSB, LPT, LBSB and LBPT from top to bottom panel in Fig. C.1., respectively.

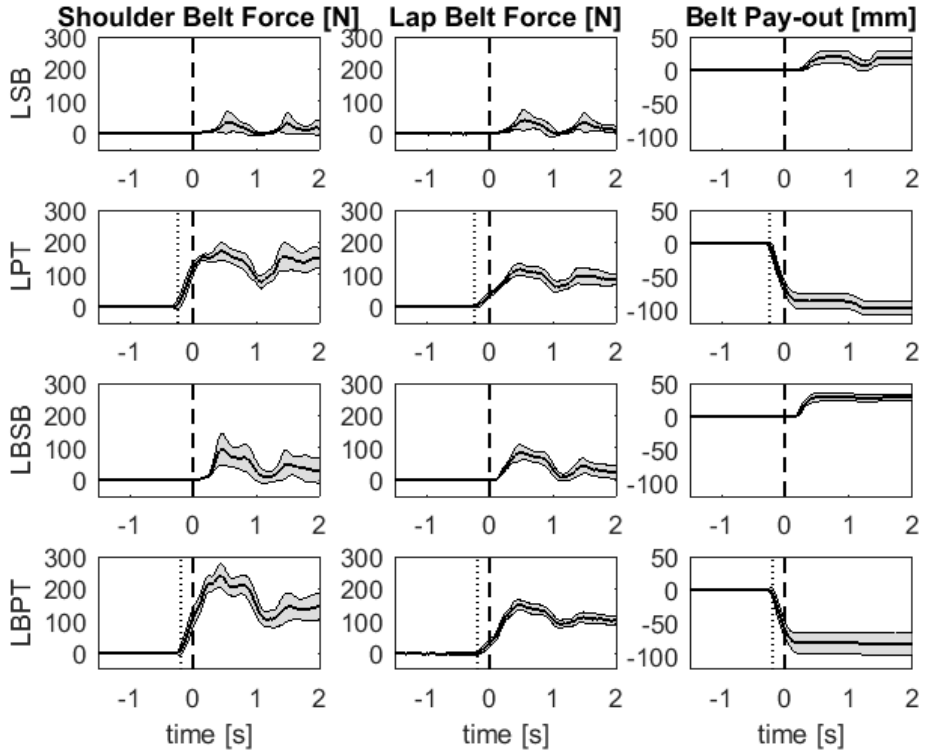

Fig. C.1. Belt forces and pay-out in LSB (n=25), LPT (n=23), LBSB (n=24) and LBPT (n=20) from top to bottom row, respectively. Vertical dashed lines present time zero and vertical dotted lines present the onset time of the pre-tensioned belt.

Appendix D

Volunteer kinematics in LPT, LBSB and LBPT are presented in Fig. D.1 to Fig. D.6.

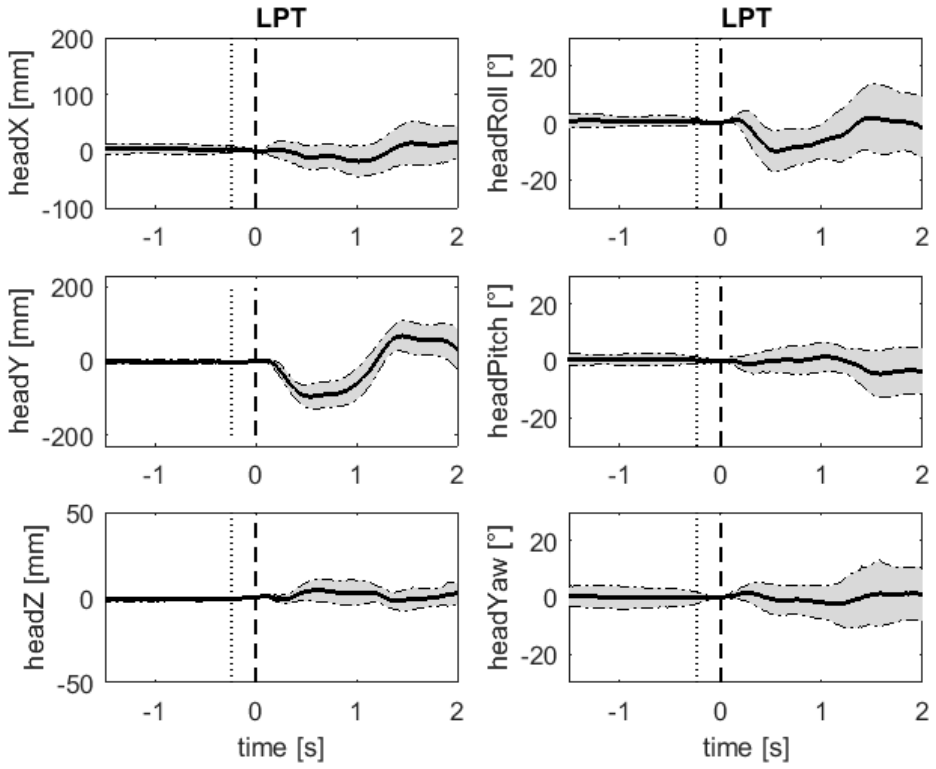

Fig. D.1. Head kinematics in LPT. Vertical dashed lines present time zero and vertical dotted lines present the onset time of the pre-tensioned belt, n=23.

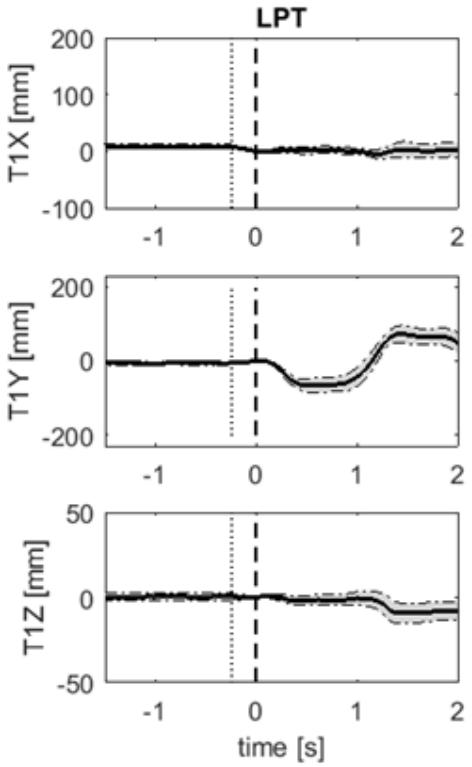

Fig. D.2. Upper torso kinematics in LPT. Vertical dashed lines present time zero and vertical dotted lines present the onset time of the pre-tensioned belt, n=23.

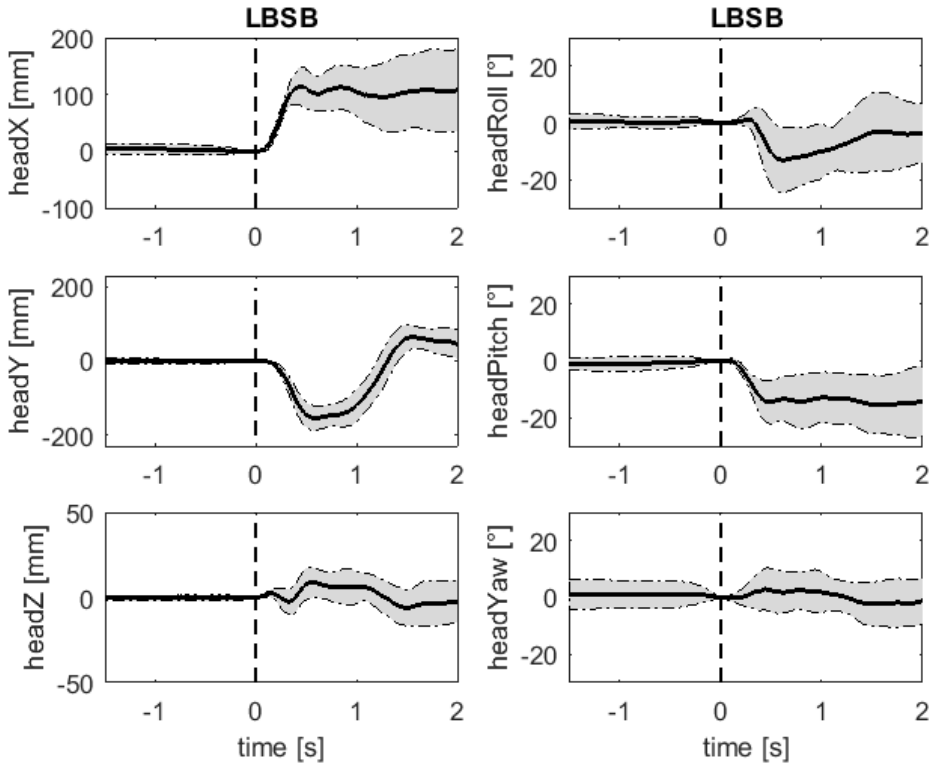

Fig. D.3. Head kinematics in LBSB. Vertical dashed lines present time zero, n=24.

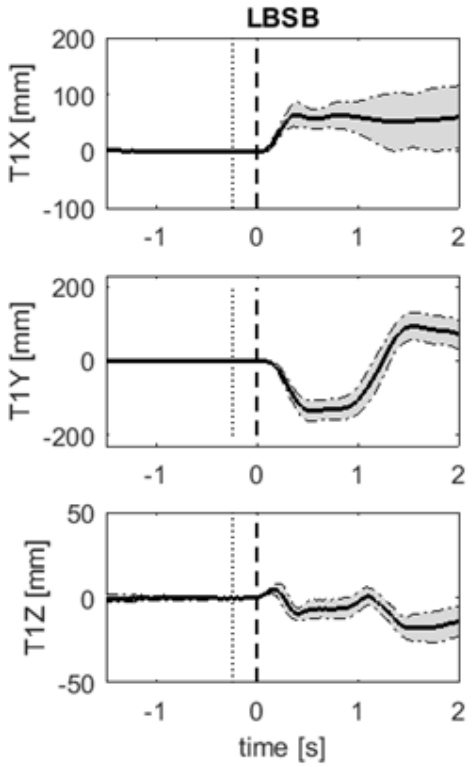

Fig. D.4. Upper torso kinematics in LBSB. Vertical dashed lines present time zero, n=24.

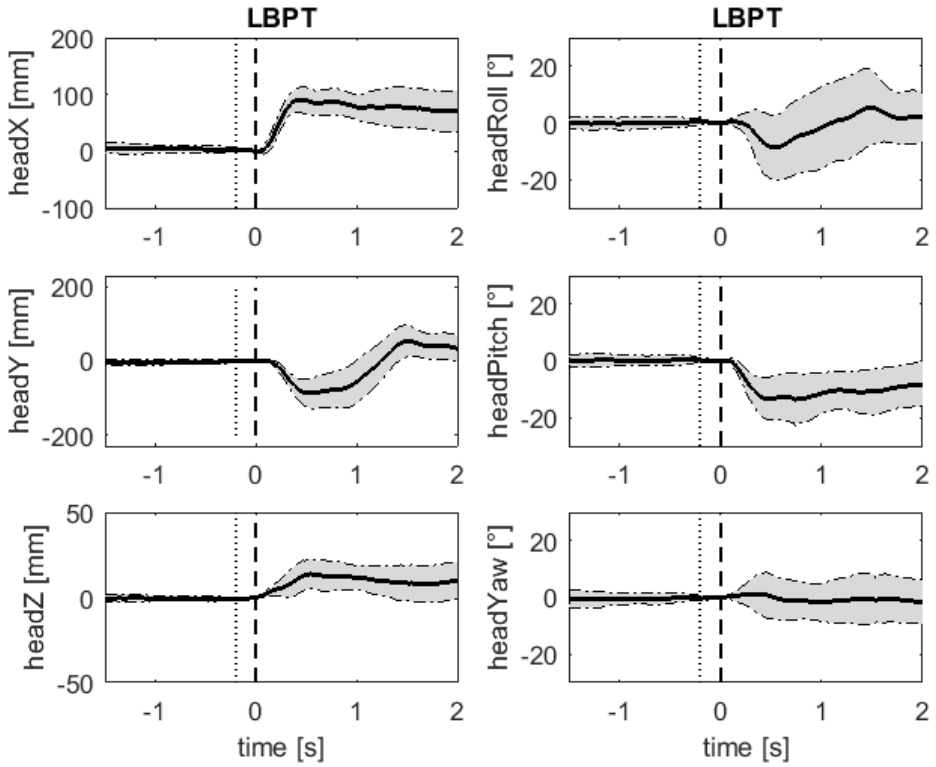

Fig. D.5. Head kinematics in LBPT. Vertical dashed lines present time zero and vertical dotted lines present the onset time of the pre-tensioned belt, n=20.

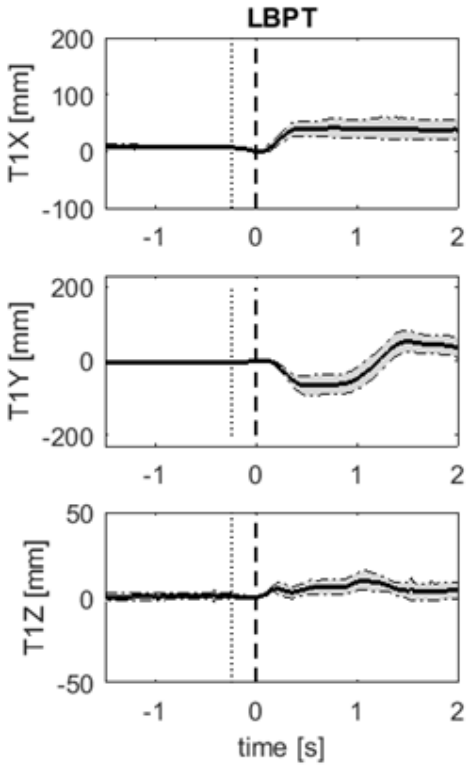

Fig. D.6. Upper torso kinematics in LBPT. Vertical dashed lines present time zero and vertical dotted lines present the onset time of the pre-tensioned belt, n=20.

Appendix E

The pressure distribution between the human body and the passenger seat is presented at five time points, for one volunteer test, in Fig. E.1.

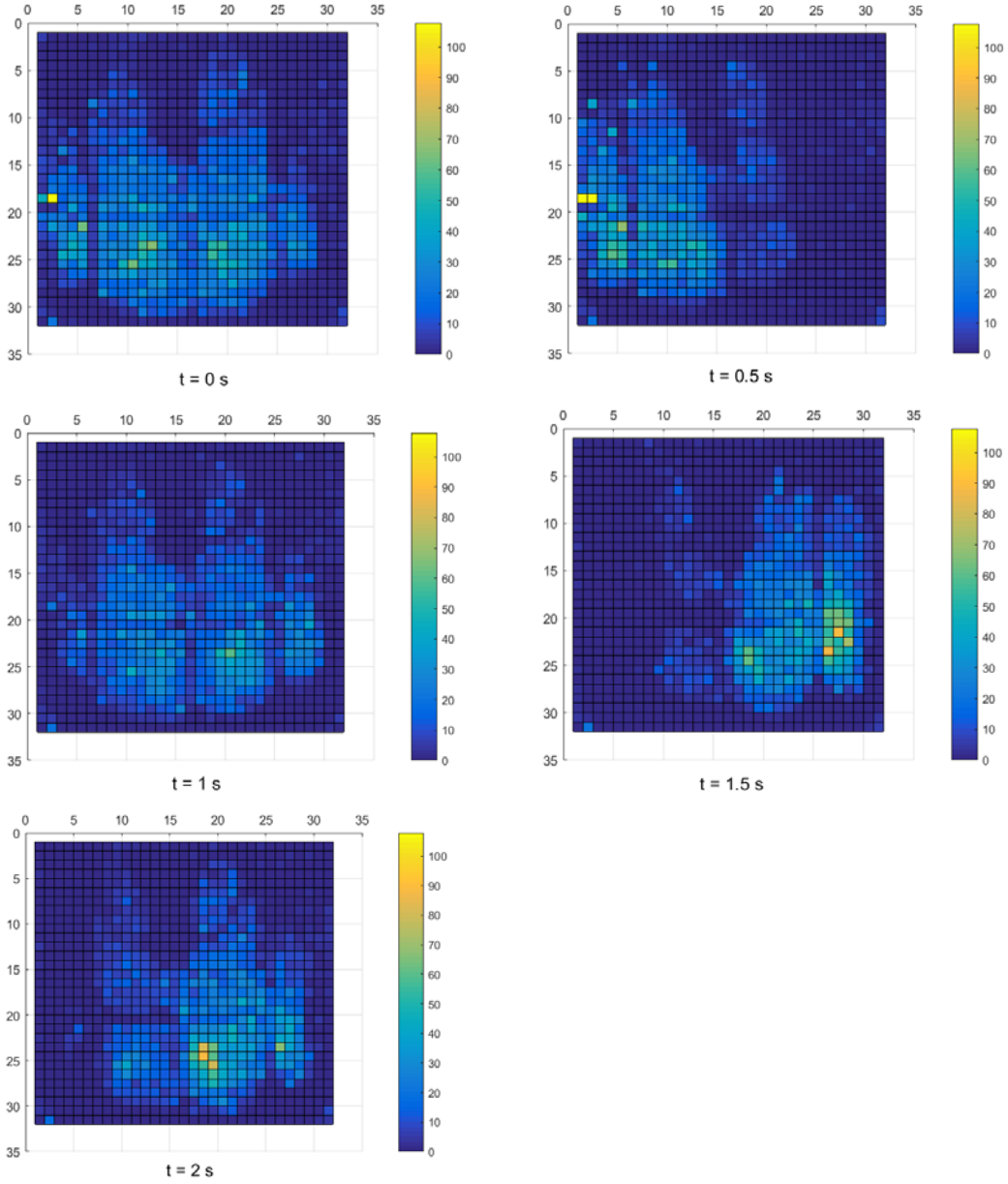

Fig. E.1. Pressure distribution on passenger seat (male 3) in one LSB manoeuvre for five points in time.